UDC 004.942:537.525
DOI: 10.20535/SRIT.2308-8893.2024.3.05

COMPARISON OF METHODS FOR INTERPOLATION AND EXTRAPOLATION OF BOUNDARY TRAJECTORIES OF SHORT-FOCUS ELECTRON BEAMS USING ROOT-POLYNOMIAL FUNCTIONS

I. MELNYK, A. POCHYNOK, M. SKRYPKA

Abstract. The article considers and discusses the comparison of interpolation and extrapolation methods of estimation of the boundary trajectory of electron beams propagated in ionized gas. All estimations have been computed using root-polynomial functions to numerically solve a differential-algebraic system of equations that describe the boundary trajectory of the electron beam. By providing analysis, it is shown and proven that in the case of solving a self-connected interpolation-extrapolation task, the average error of the beam radius estimation is generally smaller. This approach was especially effective in estimating the focal beam radius. An algorithm for solving self-connected interpolation-extrapolation tasks is given, and its efficiency is explained. Corresponding graphic dependencies are also given and analyzed.

Keywords: interpolation, extrapolation, root-polynomial function, ravine function, average error, electron beam, boundary trajectory.

INTRODUCTION

The development of electron beam technologies is very important today for advanced branches of industry, including metallurgy, mechanical engineering, instrument making, and microelectronic production, as well as automotive, aircraft, and space industries [1–10]. It is caused by the advantages of the electron beam as a technological instrument, such as its high total power and power density, the simplicity of changing and controlling focal beam parameters using electric and magnetic fields, as well as providing technological operation in the medium of pure vacuum [1–10].

For example, the use of electron beams today in the electronic industry is mostly oriented toward welding contacts of electronic devices, including cryogenic ones [8–12], deposition of ceramic dielectric films for high-quality capacitors and microwave transmitters and receiver devices [9; 10; 13–15], as well as toward refining of silicon [16–19]. A special technical problem is obtaining and applying intensive electron beams in high-energy accelerators [7; 20–22].

In such circumstances, the development of electron beam technologies and the sources of electrons are provided in two main directions. The first is improving the traditional electron guns with heated cathodes, and the second is the elaboration of novel types of electron sources based on other physical principles. For example, electron sources based on gas discharges are elaborated today and successfully applied in industry.

Among this type of electron source, a special place occupied the high-voltage glow discharge (HVGD) electron guns, which are generally characterized by the stable operation in the soft vacuum in the medium of different gases, including active and noble ones, as well as by simplicity of construction [23–28]. Another well-known advantage of HVGD electron guns is their simplicity in controlling discharge current and beam power. In the paper [29], the slow aerodynamic control of HVGD current using electromagnetic valves has been considered, and the corresponding time regimes have been analyzed. Fast electric control of beam power by lighting the additional low-voltage discharge and changing the concentration of charged particles in anode plasma, as well as the corresponding time regimes for such fast regulation, have been considered in the paper [30].

Generally, the main advantage possibilities for using HVGD electron guns in industry are as follows:

1. Refining of silicon for the microelectronic industry [16–20; 31].
2. Obtaining high-quality ceramic films for microelectronic production and for power-energetic insulators. Obtaining defense films for cutting instruments and heat-protection films for engines in the automotive, aircraft, and space industries by applying HVGD electron guns is also possible [33–37].
3. Development of 3-D printing technology by metals [38–40].

Therefore, in such circumstances, the development of novel mathematical approaches for the simulation of short-focus electron beams generated by HVGD electron guns is generally necessary.

PERVIOUS RESEARCHES AND STATEMENT OF THE SIMULATION PROBLEM

The problem is that today elaboration of HVGD electron guns is mostly provided by a combination of sophisticated theoretical approaches [23; 26–30] and complex experimental works [24; 25], because simplified mathematical relations for estimation of the focal parameters of short-focus electron beams at low pressure in ionized gas don't exist [23]. Also, in part of the book [23], general approaches for the simulation of electric field distribution and the trajectories of charged particles have been systematized. Corresponding recommendations for the simulation of HVDG electron guns have also been given in [23]. But in any case, such a sophisticated approach to designing this type of guns is significantly hinders the necessary development and implementation in industry of its novel, advanced constructions. Therefore, the finding of simplified mathematical relations for interpolation, extrapolation, and approximation of the trajectories of short-focus electron beams in low-pressure ionized gas is necessary [23]. Corresponding relations for an intensive long-focus electron beam propagated in high vacuum in ion-

ized gases are well-known [1–10]. In the paper [41], simple analytical relations for estimating the depth of welding seam penetration using short-focus electron beams formed by HVGD electron guns have been proposed. Corresponding simulation results have been analyzed and compared with experimental data [41]. Therefore, it is clear that finding and analyzing the simple analytical relations for estimation of the focal parameters of short-focus electron beams propagated in ionized gas is really necessary.

In the years 2019–2020 in the papers [42–44] a simple approach for estimating the parameters of short-focus electron beams propagated in ionized gas has been proposed. Generally, this approach is based on the suggestion that, in such physical conditions, the beam boundary trajectory can be described with high precision by the ravine function, which has one global minimum, and outside the region of minimum, this dependence is similar to a linear one. Such an approach generally corresponds to the main singularities of the physics of electron beams [1–10]. In the papers [42–44], by the numerical experiments have shown that such ravine functions with the precision of fractions of a percent can be described by root-polynomial functions, written as follows [42–45]:

$$r_b(z) = \sqrt[n]{C_n z^n + C_{n-1} z^{n-1} + \ldots + C_1 z + C_0}, \tag{1}$$

where z is the longitudinal coordinate of beam propagation, $r_b(z)$ is the beam radius in corresponded cross-section by z coordinate, n is the degree of the polynomial and the order of the root-polynomial function, and $C_0 \ldots C_n$ are the polynomial coefficients.

The generally obtained results of interpolation have been systematized and analyzed in the paper [45]. In this work, analytical relations for calculation of the coefficients of root polynomial functions (1) from second to fifth order n have been obtained, and the interpolation task was solved relatively to numerical solution of the corresponded set of algebra-differential equations, which described the boundary trajectory of an electron beam propagated in ionized gas [1–10; 23; 45]:

$$f = \frac{n_e}{n_{i0} - n_e};\ C = \frac{I_b(1 - f - \beta^2)}{4\pi\varepsilon_0 \sqrt{\frac{2e}{m_e}} U_{ac}^{1.5}};\ \frac{d^2 r_b}{dz^2} = \frac{C}{r_b};\ \theta = \frac{dr_b}{dz} + \theta_s;$$

$$n_e = \frac{I_b}{\pi r_b^2};\ \ v_e = \sqrt{\frac{2eU_{ac}}{m_e}};\ \ n_{i0} = r_b^2 B_i p n_e \sqrt{\frac{\pi M \varepsilon_0 n_e}{m_e U_{ac}}} \exp\left(-\frac{U_{ac}}{\varepsilon_0 n_e r_b^2}\right);$$

$$\gamma = \sqrt{1-\beta^2};\ \tan\left(\frac{\theta_{\min}}{2}\right) = \frac{10^{-4} Z_a^{4/3}}{2\gamma\beta^2};\ \tan\left(\frac{\theta_{\max}}{2}\right) = \frac{Z_a^{3/2}}{2\gamma\beta^2}; \tag{2}$$

$$\overline{\theta^2} = \frac{8\pi (r_b Z_a)^2 dz}{n_e} \ln\left(\frac{\theta_{\min}}{\theta_{\max}}\right),\ \ \beta = \frac{v_e}{c},$$

where U_{ac} is the accelerating voltage, I_b is the electron beam current, p is the residual gas pressure, z is the longitudinal coordinate, r_b is the radius of the

boundary trajectory of the electron beam, n_e is the beam electrons' concentration, n_{i0} is the concentration of residual gas ions on the beam symmetry axis, m_e is the electron mass, f is the residual gas ionization level, B_i is the gas ionization level, ε_0 is the dielectric constant, v_e is the average velocity of the beam electrons, c is the light velocity, γ is the relativistic factor, $\theta_{\min}$ and $\theta_{\max}$ are the minimum and maximum scattering angles of the beam electrons, corresponding to Rutherford model [1–10], Z_a is the nuclear charge of the residual gas atoms, dz is the length of the electron path in the longitudinal direction at the current iteration, and $\bar{\theta}$ is the average scattering angle of the beam electrons.

In the work [45], it has also been proven that the ravine function (1) can be successfully used for interpolation of the results of solving the set of equations (2) with very small errors in the range of 0.1–8%. Corresponding dependences of interpolation error on z coordinates are given in Fig. 1 [45]. But the main conclusion that has been made is that interpolation error strongly depends on the position of the base points of interpolation, whose number is always equal to $n+1$. Generally, the ravine function, which is described by a set of relations (2), is always symmetric relatively to the plane $z = z_f$, where z_f is the location of beam focus, which should correspond to the minimum of the ravine root-polynomial function (1) [1–10]. Therefore, in [45], the symmetric position of the base point, which gives the minimal error of interpolation, has been considered. When the numerical solution is asymmetric, the error of interpolation is usually increasing several times [45]. Such estimations of asymmetric solutions also increase the error in defining focal beam parameters.

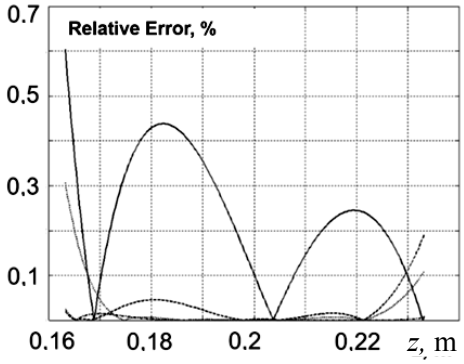

Fig. 1. Errors of interpolation of the boundary trajectory of the electron beam depend on *z* coordinate [45]

The solid line corresponded to a second-order function, the dotted line — to a third-order function, the dashed line — to a fourth-order function, and the dash-dotted line — to a fifth-order function. Model parameters: $U_{ac} = 10\,\text{kV}$; $I_b = 0.5\,\text{A}$; $p = 0.1\,\text{Pa}$.

Therefore, the transformation of the asymmetric dataset for solving the set of relations (2) into a symmetric one has been proposed, and the corresponding simulation results have been studied. In such conditions, the additional symmetric point is given to the analyzed data set, and the task of interpolation with defining the polynomial coefficients $C_0 \ldots C_n$ is solved between two symmetric points. And outside this symmetric region, the task of extrapolation for the same root-

polynomial function (1) has been solved, and the corresponding total error of interpolation and approximation has been defined. The general formulation of this task and the analysis of the obtained simulation results are given in the next sections of this article.

In the paper [46], the possibility of using third-order root-polynomial functions for approximation experimental data about the boundary trajectories of short-focus electron beams in ionized gases as well as the corresponding algorithm of approximation has been considered. Another approach for the simulation of gas discharge electron beam devices with consideration of experimental data has been proposed in the paper [20].

The provided analysis of relevant sources on methods of interpolation and extrapolation showed that other known methods for estimation of the ravine functions either give a large error or are generally not suitable for solving the problem of estimation boundary trajectories of electron beams [42–50]. For example, for polynomial interpolation and extrapolation [48; 49], eliminating unnecessary outliers of the estimated data, especially for high-order polynomials, is generally impossible. Such an estimate, with the exception of a large error, does not even provide sufficiently reliable qualitative results about the boundary trajectory of the electron beam. As a rule, the reason for these outliers is different values of the derivative of the ravine function in the region of the minimum and outside it. The main advantages of the proposed approach of interpolation using root-polynomial functions are as follows:

1. The smoothing of the estimated root-polynomial function in the region of linear variation of numerical data.

2. Obtaining, by this reason, only one global minimum in corresponded area.

Generally, even for high-order root-polynomial functions, outliers and unnecessary extremums are not observed [45].

It is for this reason that the interpolation error is significantly smaller, especially for the symmetrical ravines data sets [45]. Therefore, the main subject of the presented research is to study the possibilities of transforming asymmetric sets of numerical data into symmetric ones using appropriate numerical methods of functional analysis [58–52].

FORMALIZING INTERPOLATION AND EXTRAPOLATION TASKS FOR ASYMMETRIC RAVINE FUNCTIONS DESCRIBED BOUNDARY TRAJECTORIES OF ELECTRON BEAM

Generally, the regions of interpolation and approximation for right-hand and left-hand asymmetric ravine data functions are shown in the Fig. 2. It is clear that the main idea of this approach is to choose the position of the boundary point z_{bp}, which divides the whole range of providing calculations by z coordinate into two regions: Interpolation Region IR and Extrapolation Region ER.

By this way, the task of calculating the boundary trajectory of an electron beam comes down to the problem of interpolation of the symmetric ravine function on the region IE, which has been considered and described in the papers [42–

45]. After that, the root-polynomial function (1) with the same coefficients is used for the Extrapolation Region ER. Considering, corresponding to Fig. 2, the values of the radiuses of Start Point SP r_{start} and End Point EP r_{end}. Also considering the full set of beam trajectory coordinates (z_i, r_i), $(i \in [1; N_P])$, where N_P is the number of calculated points, has been obtained using a set of equations (2). In practice, the value of N_P is $N_P > 10^4$. On the contrary, the value of the basic points N_{BP} for solving complex interpolation-extrapolation tasks is significantly smaller: $N_{BP} = n - 1$. Also, i_0, the start value of variable i, is necessary to formalize the considered task by numerical algorithm. Using the previously described assumptions, the position of the boundary point z_{bp} is defined by following the recurrent arithmetic-logic relation [47]:

$$z_b(i) = (r_{end} > r_{start}) \cdot \left(\begin{pmatrix} r(i) < r_{start} \\ i_0 = 1;\ i = i + 1 \end{pmatrix} \cdot z(i) + \begin{pmatrix} r(i) \geq r_{start} \\ i = i + 1 \end{pmatrix} \cdot z_b(i-1) \right) +$$

$$+ (r_{start} \geq r_{end}) \cdot \left(\begin{pmatrix} r(i) < r_{end} \\ i_0 = N_P;\ i = i - 1 \end{pmatrix} \cdot z(i) + \begin{pmatrix} r(i) \geq r_{end} \\ i = i - 1 \end{pmatrix} \cdot z_b(i+1) \right). \qquad (3)$$

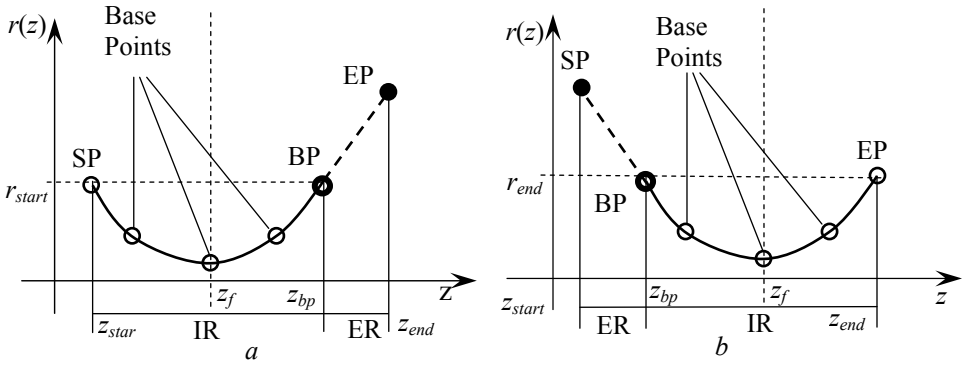

Fig. 2. Right-hand (*a*) and left-hand (*b*) asymmetric ravine functions: IR — Interpolation Region; ER — Extrapolation Region; SP — Start Point; EP — End Point; BP — Boundary Point

The formalized algorithm for solving the complex self-connected interpolation-extrapolation task using relation (1)–(3) on the different regions of longitudinal coordinate z is described by the flowchart presented in Fig. 3.

SOFTWARE FOR NUMERICAL EXPERIMENTS AND ESTIMATIONS OF ERRORS

Using the algorithm described in the previous section of the article for finding the boundary point z_b, both interpolation and self-connected interpolation-extrapolation tasks have been solved. After that, the error of estimation was analyzed. Both tasks are solved in the region $z \in [z_{\min}, z_{\max}]$. Such types of errors were considered and analyzed.

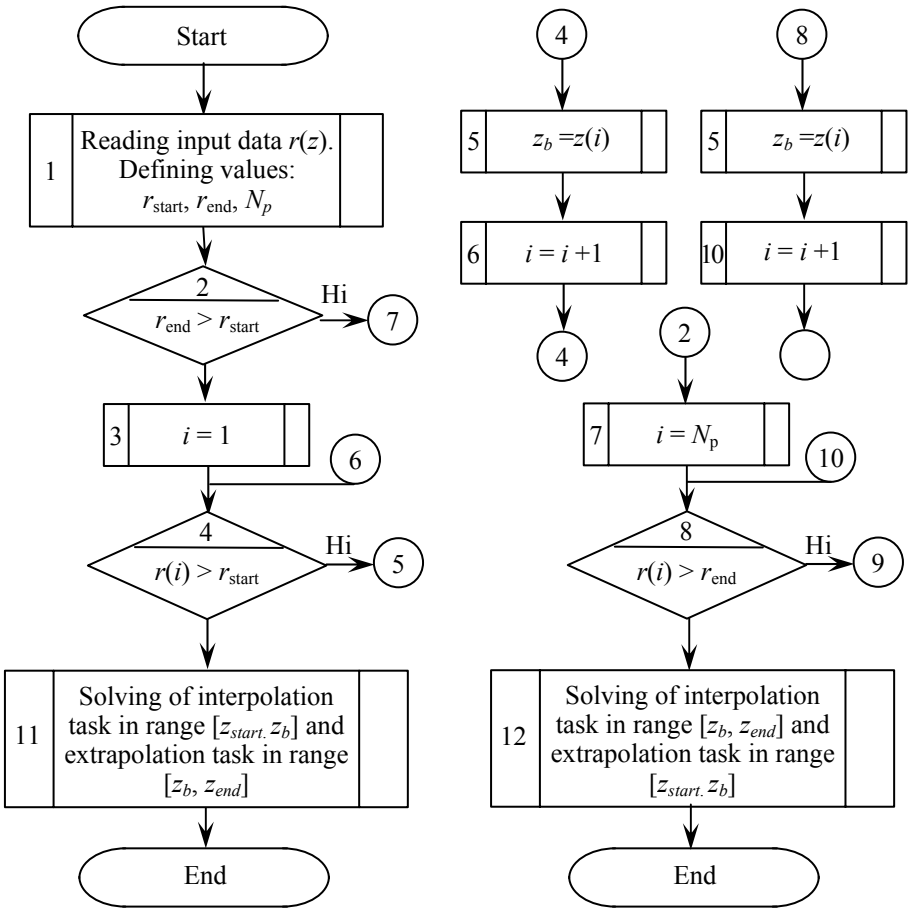

Fig. 3. Flowchart of considered algorithm for solving self-connected interpolation-extrapolation task

1. Maximal error $\varepsilon_{\max}$.

2. Average error ε_{av}, which is generally defined by the well-known method of optimization technique [48–52] and of mathematical statistics [53; 54] as follows:

$$\varepsilon_{av} = \frac{\sum_{i=1}^{N_p} |r_{est} - r_{sim}|}{N_p},$$

where r_{sim} is the radius of the electron beam, calculated numerically by the set of equations (2) using the fourth-order Runge-Kutt method [51; 52], and r_{est} is the value of the beam radius, estimated using relation (2).

3. Error on focus position ε_F.

4. Error on focal beam radius ε_{rf}.

Corresponding relations for defining the third and fourth types of errors have been considered in the papers [43–45].

Corresponding software for the simulation and estimation parameters of electron beams was realized in the Python programming language, including advanced libraries for scientific calculations and graphic libraries. For the correct

location and including these libraries, a virtual environment, virtual memory, virtual variables, and virtual disk have been created on the local computer [55; 56].

Let's consider some results of the simulation and errors in estimations.

Task 1. Acceleration voltage U_{ac} is 15 kV; beam current I_b is 8.5 A; operation pressure in the guiding channel p is 4.5 Pa; the initial radius of the electron beam r_{start} is 8.5 mm; the initial angle of convergence of the electron beam θ is 15^0; the starting point z_{start} is 0.1 m; the first end point z_{end} is 0.15 m; and symmetrical point z_b with the same radius is 0.148 m. That is, the length of the symmetrical segment for the highest interpolation accuracy: $0.148\,\text{m} - 0.1\,\text{m} = 0.048$ m.

For this example, dependence $r(z)$, defined using the set of equations (2), is presented in Fig 4.

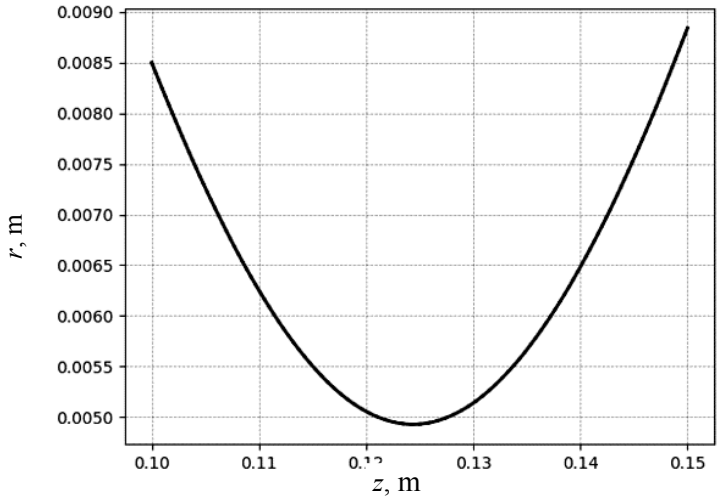

Fig. 4. Dependence *r*(*z*) for $U_{ac} = 15\,\text{kV}$, $I_b = 8.5\,\text{A}$, $p = 4.5\,\text{Pa}$, end point $z_{\text{end}} = 0.15\,\text{m}$ (screen copy)

It is clear that the dependence presented in Fig. 4 is a right-hand asymmetric ravine function. Errors in solving interpolation and self-connected interpolation-extrapolation tasks for this example are presented in Table 1. All errors have been estimated for different order of root-polynomial functions n and length of extrapolation region L_{add}. Task parameter L_{add} is given in Table 1 in absolute value, in meters, and relatively to the length of the interpolation region IR, in percents.

The dependences of estimation errors for two fourth-order root-polynomial functions that have been obtained for solving interpolation and self-connected interpolation-extrapolation tasks are presented in Fig. 5. It is clear that the level of maximal error is similar, nearly 3%, but in the case of extrapolation error in the focal region, it is generally smaller. Corresponding data from Table 1 are as follows; interpolation: $\varepsilon_F = 0.06\,\%$, $\varepsilon_{rf} = 7.56 \cdot 10^{-3}\,\%$; extrapolation: $\varepsilon_F = 0.0041\,\%$, $\varepsilon_{rf} = 1.82 \cdot 10^{-6}\,\%$. Data from Table 1 show also that if for the extrapolation task the maximal error value $\varepsilon_{\max}$ can be greater, then in the case of interpolation, the value of the average error for the extrapolation task ε_{av} is generally smaller. The dependences of the value of ε_{av} on the relative length of the extrapolation region ER for the tasks of interpolation and self-connected interpolation-extrapolation are presented at Fig. 6.

Table 1. Interpolation and extrapolation errors for Task 1

n	$\varepsilon_{\max}$, %		ε_{av}, %		ε_F, %		ε_{rf}, %		L_{add}, m / %
	Extrapolation	Interepolation	Extrapolation	Interepolation	Extrapolation	Interepolation	Extrapolation	Interepolation	
2	2.29	2.84	1.26	1.4476	0	0.08	$5.28\cdot10^{-13}$	$1.7\cdot10^{-3}$	$2\cdot10^{-3}$ / 4.2
3	5.92	6.58	3.25	3.55	0	0.02	0.6	0.635	
4	0.66	0.844	0.2734	0.31	0	0.004	$7.7\cdot10^{-11}$	$2.1\cdot10^{-4}$	
5	2.08	2.27	0.85	0.925	0	0.004	0.44	0.47	
6	0.14	0.203	0.063	0.07	0	0.02	$2.4\cdot10^{-8}$	$8.5\cdot10^{-5}$	
2	2.3	3.243	1.25	1.546	$1.11\cdot10^{-14}$	$6\cdot10^{-3}$	$4.57\cdot10^{-13}$	$6\cdot10^{-3}$	$3\cdot10^{-3}$ / 6.25
3	5.914	7.14	3.2	3.76	0	0.0041	0.629	$7.6\cdot10^{-3}$	
4	0.649	1.0	0.27	0.34	0.0041	0.06	$1.82\cdot10^{-6}$	$7.56\cdot10^{-3}$	
5	2.2	2.58	0.884	1.03	0.0041	0.02	0.48	0.53	
6	0.27	0.256	0.084	0.0654	0	0.041	$3.51\cdot10^{-9}$	$4\cdot10^{-4}$	
2	2.3	3.7	1.254	1.66	0	0.22	$1.23\cdot10^{-13}$	0.013	$4\cdot10^{-3}$ / 8.3
3	5.9	7.71	3.197	3.973	0	$4.1\cdot10^{-3}$	0.65	0.744	
4	0.86	1.17	0.2765	0.38	0.0042	0.1	$7.1\cdot10^{-7}$	$1.878\cdot10^{-3}$	
5	2.33	2.93	0.93	1.14	0.0042	0.6	0.52	0.03345	
6	0.424	0.316	0.07	0.1	0	0.067	$2.23\cdot10^{-8}$	10^{-3}	
2	2.29	4.113	1.27	1.782	$2.23\cdot10^{-14}$	0.291	$2.46\cdot10^{-13}$	0.0224	$5\cdot10^{-3}$ / 10.4
3	5.9	8.3	3.2	4.195	0	$85\cdot10^{-3}$	0.68	0.8	
4	1.15	1.35	0.288	0.4264	0	0.14	$3.38\cdot10^{-11}$	$3.86\cdot10^{-3}$	
5	2.474	3.311	1.0	1.2646	0.0043	0.047	0.5637	0.67	
6	0.56	0.383	0.08	0.1166	0	$9.376\cdot10^{-2}$	$2\cdot10^{-8}$	$2\cdot10^{-3}$	
2	4.89	6.6	1.4573	2.6	$1.11\cdot10^{-14}$	0.676	$4.39\cdot10^{-13}$	0.1263	10^{-2} / 20.8
3	9.52	11.3	3.5	5.4	0	0.02	0.8	1.1443	
4	2.97	2.45	0.42	0.76	0	0.44	$6.35\cdot10^{-11}$	$3.56\cdot10^{-2}$	
5	4.17	5.9	1.39	2.07	$4.7\cdot10^{-3}$	1.77	0.812	1.1226	
6	1.69	0.83	0.17	0.2756	0	0.34	$1.12\cdot10^{-8}$	0.0273	

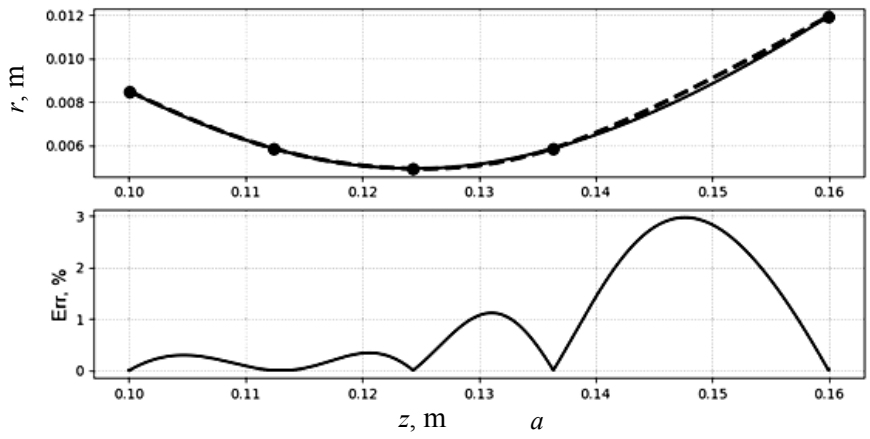

Fig. 5. Dependences of electron beam radius (top) and error of estimation (bottom) on z coordinate for the interpolation task (*a*) and the self-connected interpolation-extrapolation task (*b*). $U_{ac} = 15\,\text{kV}$; $I_b = 8.5\,\text{A}$; $p = 4.5\,\text{Pa}$; $n = 4$; $z_{\text{end}} = 0.16\,\text{m}$. On the top dependence $r(z)$, the straight line corresponds to the obtained numerical solution, and the dash line corresponds to estimations (screen copy)

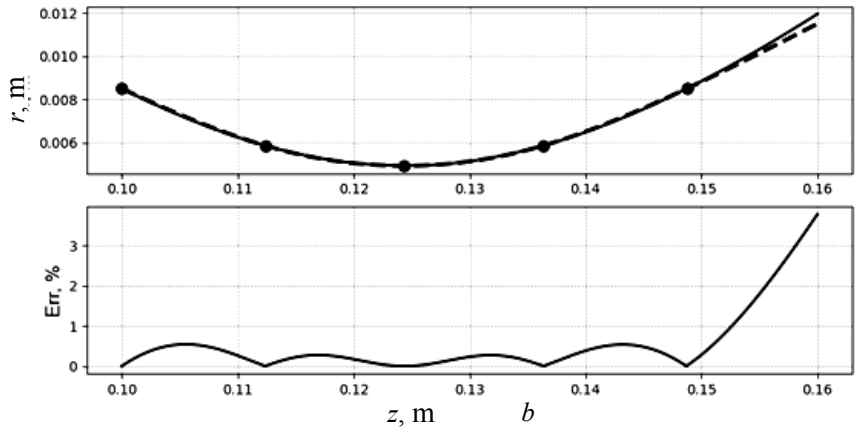

Contiued Fig. 5

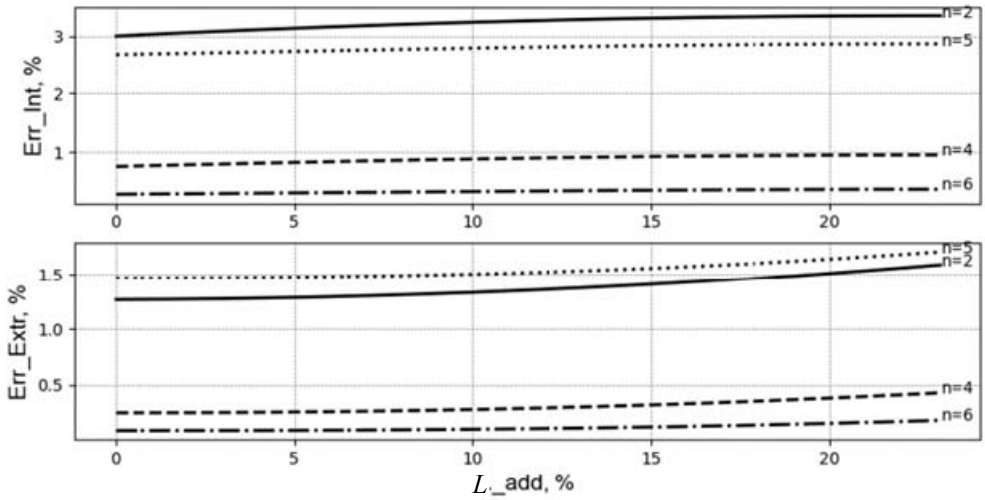

Fig. 6. Dependences of average error ε_{av} of interpolation (top) and end interpolation-extrapolation (bottom) tasks on the value of extrapolation region ER relative to interpolation region IR L_{add} for the root-polynomial functions of different order n. Right-hand ravine function, Task 1 (screen copy)

Task 2. U_{ac} is 15 kV; I_b is 5.5 A; p is 4.5 Pa; r_{start} is 10.3 mm; θ is 15^0; z_{start} is 0.1 m; and z_{end} is 0.15 m. Since in this case $r_{start} > r_{end}$, symmetrical point z_b with the same radius, as r_{end}, is $z_b = 0.101743$ m. That is, the length of the symmetrical segment for the highest interpolation accuracy:

$$0.147\text{ m} - 0.101743\text{ m} = 0.045257\text{ m},\ \text{or, in relative units:}$$

$$0.001743\text{ m} / 0.045257\text{ m} \cdot 100\,\% = 3.85\,\%.$$

In the next steps of providing the calculations, we will reduce the coordinate z_{end} of the end point of the considered interval. That is, take $z_{end} < 0.147$. Thus, we bring it closer to the extremum of the $r(z)$ ravine function, or to the position of the focus of the electron beam z_f. In this way, we will decrease the interpolation interval IR and increase the extrapolation interval ER. For this task, dependence $r(z)$, defined using the set of equations (2), is presented in Fig 7.

It is clear that the dependence presented in Fig. 7 is a left-hand asymmetric function. Errors in solving interpolation and self-connected interpolation-extrapolation tasks for this example are presented in Table 2.

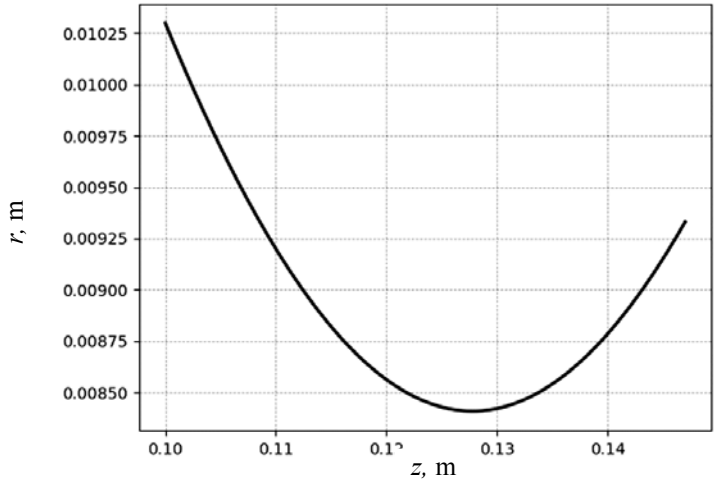

Fig. 7. Dependence $r(z)$ for $U_{ac} = 15\,\text{kV}$, $I_b = 8.5\,\text{A}$, and end point $z_{\text{end}} = 0.147\,\text{m}$ (screen copy)

Table 2. Interpolation and extrapolation errors for Task 2

n	$\varepsilon_{\max}$, %		ε_{av}, %		ε_F, %		ε_{rf}, %		L_{add}, m / %
	Extrapo-lation	Interepo-lation	Extrapo-lation	Interepo-lation	Extrap-olation	Interepo-lation	Extrapo-lation	Interepo-lation	
2	1.85	2.5215	1.0	1.224	0	0.1	$6.68\cdot10^{-13}$	$2.86\cdot10^{-3}$	$1.75\cdot10^{-3}$/ 3.8
3	4.8	5.6522	2.6	2.98	0	$3.77\cdot10^{-3}$	0.46	0.5	
4	0.497	0.7	0.2	0.247	0	$2.34\cdot10^{-4}$	$6.37\cdot10^{-11}$	0.034	
5	1.4255	1.624	0.593	0.6754	0	$7.56\cdot10^{-3}$	0.29	0.317	
6	0.1716	0.1737	$4.236\cdot10^{-2}$	$5.31\cdot10^{-2}$	0	$2\cdot10^{-2}$	$1.6\cdot10^{-8}$	$9.1\cdot10^{-3}$	
2	1.6	2.6	0.88	1.1743	$1.11\cdot10^{-14}$	0.16	$1.4\cdot10^{-13}$	$6.5\cdot10^{-3}$	$2.75\cdot10^{-3}$/ 6.35
3	4.2	5.51	2.27	2.81	0	$3.7\cdot10^{-2}$	0.4	0.45	
4	0.583	0.752	0.1722	0.236	0	$5\cdot10^{-2}$	$3.69\cdot10^{-12}$	$5.16\cdot10^{-4}$	
5	1.19	1.74	0.5	0.61	0	$7\cdot10^{-3}$	0.243	0.2764	
6	0.26	0.19	0.037	0.05	0	0.026	$1.53\cdot10^{-8}$	$1.55\cdot10^{-4}$	
2	1.686	2.68	0.782	1.1378	0	0.21	$2.28\cdot10^{-13}$	0.0112	$3.75\cdot10^{-3}$/ 9.1
3	3.6427	5.36	1.9842	2.65	0	$7.2\cdot10^{-3}$	0.346	0.41	
4	0.78	0.78	0.152	0.23	0	$6.5\cdot10^{-2}$	$8.73\cdot10^{-11}$	$8.26\cdot10^{-4}$	
5	1.13	1.3256	0.43	0.55	0	$7.236\cdot10^{-3}$	0.2	0.24	
6	0.3422	0.2	0.0343	0.05	0	$3.26\cdot10^{-2}$	$1.33\cdot10^{-9}$	$2.1\cdot10^{-4}$	
2	2.46	2.8	0.64	1.1	$1.11\cdot10^{-14}$	0.3	$6.68\cdot10^{-13}$	$2.262\cdot10^{-2}$	$5.75\cdot10^{-3}$/ 15.43
3	4.94	2.36	1.576	5.1	0	10^{-2}	0.256	0.337	
4	1.17243	0.8332	0.14	0.2293	$3.4\cdot10^{-3}$	$1.33\cdot10^{-3}$	$5.62\cdot10^{-7}$	$8\cdot10^{-2}$	
5	1.735	1.07	0.3427	0.46	0	10^{-2}	0.134	0.18	
6	0.527	0.235	$3.77\cdot10^{-2}$	$5.1\cdot10^{-2}$	0	$3.46\cdot10^{-2}$	$3.93\cdot10^{-13}$	$2.72\cdot10^{-4}$	
2	4.224	3.0	0.65	1.225	$3.34\cdot10^{-14}$	0.44	$2.81\cdot10^{-13}$	$4.74\cdot10^{-2}$	$1.075\cdot10^{-2}$ / 39.4
3	8.42	4.34	1.4	1.83	0	0.012	0.105	0.1915	
4	2.1	0.934	0.22	0.27	$3.1\cdot10^{-3}$	$8.6\cdot10^{-2}$	$7.65\cdot10^{-7}$	$1.45\cdot10^{-3}$	
5	3.354	0.86	0.39	0.327	0	$1.2\cdot10^{-2}$	$4\cdot10^{-2}$	$8\cdot10^{-2}$	
6	1.235	0.31	0.12	$6.9\cdot10^{-2}$	$3.1\cdot10^{-3}$	$3.1\cdot10^{-2}$	$3.81\cdot10^{-6}$	$2.15\cdot10^{-4}$	

The dependences for estimation error for fourth-order root-polynomial functions for interpolation and self-connected interpolation-extrapolation tasks are presented in Fig. 8. It is clear that the level of maximal error for the task of interpolation is $\varepsilon_{\max} = 0.05\,\%$, and for the self-connected interpolation-extrapolation task, it is twice as high, $\varepsilon_{\max} = 0.1\,\%$. But in this case, as in the previous example, the extrapolation error in the focal region is generally smaller. The corresponding data from Table 2 are as follows. Interpolation: $\varepsilon_F = 2.34 \cdot 10^{-4}\,\%$, $\varepsilon_{rf} = 0.034\,\%$; extrapolation: $\varepsilon_F = 0\,\%$, $\varepsilon_{rf} = 6.37 \cdot 10^{-11}\,\%$. In this task, the value of the average error for extrapolation ε_{av} is also generally smaller. The dependences of the value of ε_{av} on the relative length of the extrapolation region ER for the interpolation and self-connected interpolation-extrapolation tasks are presented in Fig. 9.

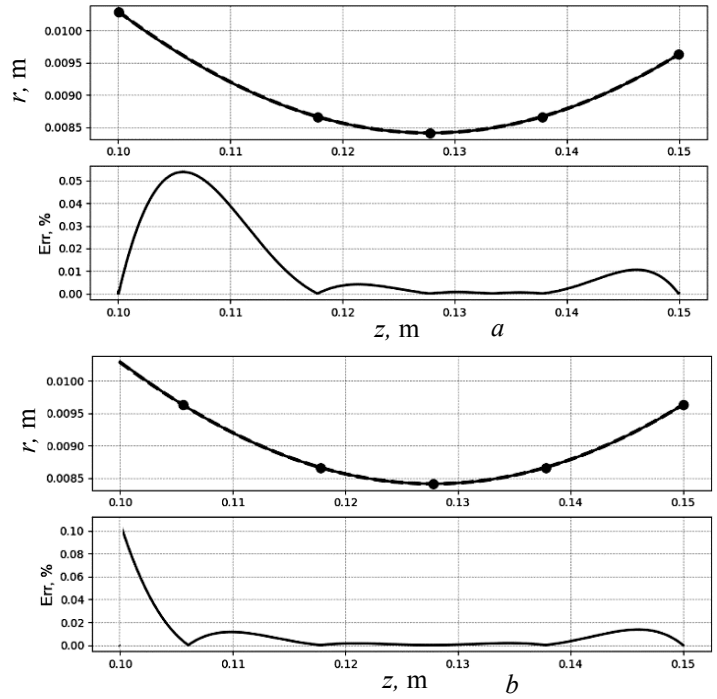

Fig. 8. Dependences of electron beam radius (top) and error of estimation (bottom) on z coordinate for the interpolation task (*a*) and the self-connected interpolation-extrapolation task (*b*). $U_{ac} = 15\,\text{kV}$; $I_b = 5.5\,\text{A}$; $p = 5.5\,\text{Pa}$; $n = 4$; $z_{\text{end}} = 0.147\,\text{m}$. On the top dependences, the $r(z)$ straight line corresponds to the obtained numerical solution, and the dash line corresponds to estimations (screen copy)

Another testing numerical experiments for right-hand and left-hand ravine numerical data, which have been provided, give the similar results of error estimation.

For the output of digital and graphic information, advanced libraries of the Python programming language have been used, such as tkinter, numpy, and matplotlib, which have been located on the virtual disk and included separately [55; 56]. A graphic interface window of elaborated software for the bookmarking "Errors of Estimation" is presented in Fig. 10. For saving and further analyzing the obtained graphic information, the bottom "Save Graph" has been provided in the interface window.

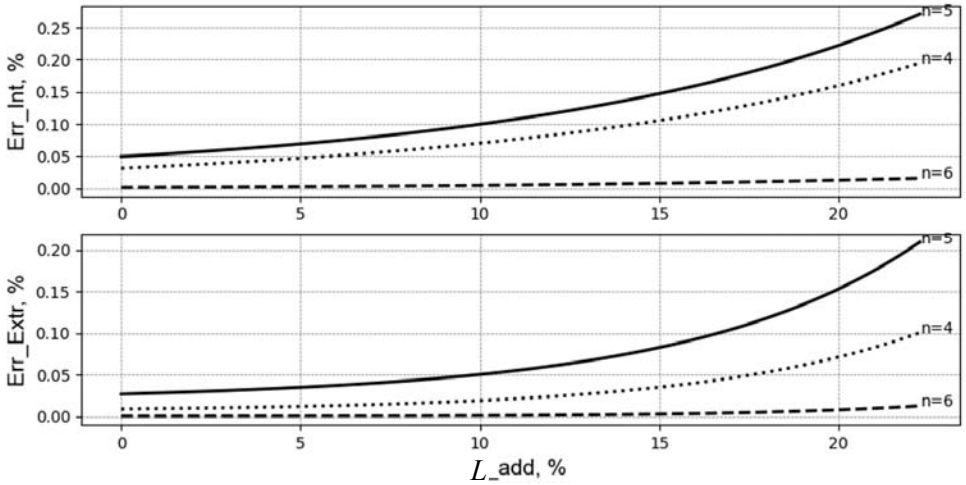

Fig. 9. Dependences of average error ε_{av} of interpolation (top) and interpolation-extrapolation (bottom) tasks on value of extrapolation region ER relative to interpolation region IR L_{add} for the root-polynomial functions of different order n. Left-hand ravine function. Task 2 (screen copy)

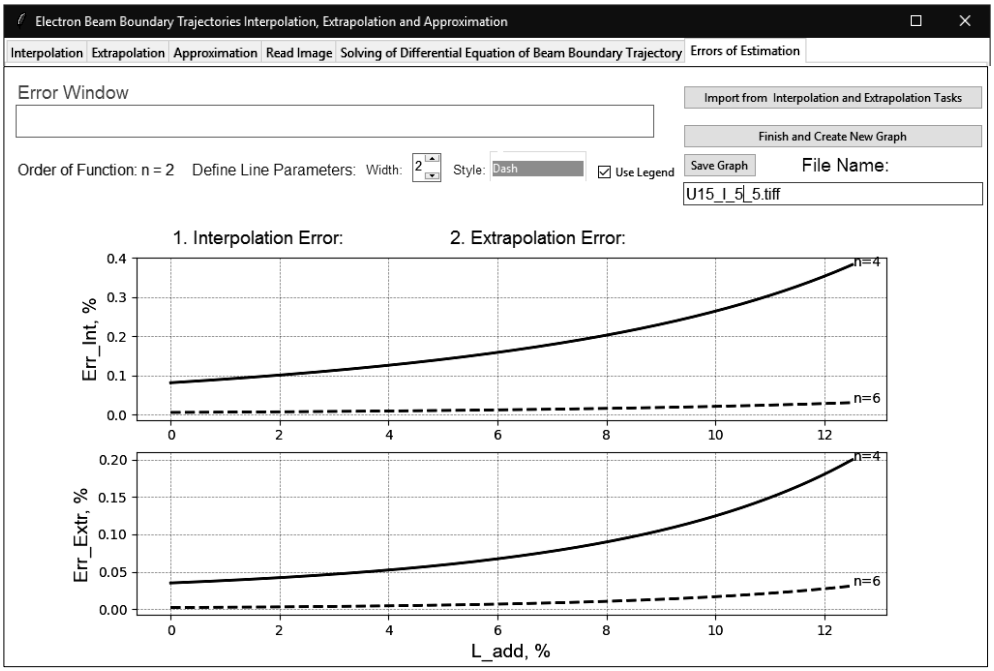

Fig. 10. Interface window for bookmarking “Errors of Estimation” in elaborated computer software

ANALYSIS OF OBTINED RESULTS AND DISCUSSION

The main conclusions about the estimation errors of interpolation and self-connected interpolation tasks are as follows:

1. Usually, the root-polynomial functions (1) of odd order have a larger error value than the functions of even order. Generally, the authors have already discussed this problem in the paper [45], and it is caused by the location of base

points. For functions of even order, the number of base points is odd, and in such a condition, one point is located in the minimum of the ravine function data, and other points are located evenly symmetrically to it. Such a location is considered optimal from the point of view of obtaining minimal interpolation error [45]. Since in the case of the odd order of the root-polynomial function and the even number of base points, this condition can't be fulfilled, the value of error, especially in the region of minimum of the ravine function, is usually greater [45]. In any case, the way to select the base points strongly influences the value of the maximal and average errors for solving interpolation and self-connected interpolation-extrapolation tasks.

2. The values of maximal and average errors for interpolation and extrapolation tasks in the cases of right-hand and left-hand asymmetric data sets are generally similar. It is generally clear by comparing the numerical data given in Table 1 and Table 2.

3. The maximal error of extrapolation increases with the enlarging of the interval of extrapolation ER L_{add}. The maximum error of extrapolation usually corresponds to the end point of this interval z_{end}. Corresponding dependences $\varepsilon_{av}(L_{add})$ are given in Fig. 6 and Fig. 9.

4. In the case of solving self-connected interpolation-extrapolation tasks, the value of the average error is generally smaller, even in cases of large values of the interval of extrapolation ER L_{add}. Corresponding digital data are given in Table 1 and Table 2.

5. In the case of solving a self-connected interpolation-extrapolation task, the values of errors in defining focal beam parameters ε_F and ε_{rf} are generally smaller. In most cases, for this task, the error of defining focus position is absent; $\varepsilon_F = 0$. Corresponding digital data are given in Table 1 and Table 2.

6. For the task of interpolation, the maximal error $\varepsilon_{\max}$ usually corresponds to the midpoint of the interval between two selected base points. Corresponding dependences $\varepsilon_{av}(z)$ are given in Fig. 5 and Fig. 8.

7. In any case, using the self-connected interpolation-extrapolation method is very effective from the point of view of obtaining the minimal error of numerical data estimation in the region of the position of the focus of an electron beam. Corresponding to Table 1 and Table 2, in some cases the error of interpolation-extrapolation estimations by the focal beam radius ε_{rf} is significantly small, resulting in a range of [10^{-13} %; 10^{-7} %].

Other features of estimating errors in solving interpolation, extrapolation, and approximation tasks for the boundary trajectory of electron beams by using root polynomial functions of the form (1), including comparison with experimental data, are the subject of separate further studies.

All research described in this paper has been provided in the Scientific and Educational Laboratory of Electron Beam Technological Devices of the National Technical University of Ukraine "Igor Sikorsky Kyiv Polytechnical Institute".

CONCLUSION

The conducted research and the obtained modeling data showed that the use of the root polynomial function (1) to solve self-connected tasks of the interpolation-extrapolation problem for ravine digital data obtained as a result of the numerical

solution of the system of algebraic-differential equations (2) and describing the boundary trajectory of a short-focus electron beam, propagating in ionized gas are very effective and provide significantly small estimation errors.

The obtained average error of estimation is in the range of $\varepsilon_{av} = 0.05 - 1.5\,\%,$ and the error of estimation of focal beam radius is in the range of $\varepsilon_F = 10^{-13} - 0.6\,\%.$ An estimations of the value of the average error on the length of the extrapolation region ER relative to the length of the extrapolation region IR are also obtained, and the corresponding graphic dependences $\varepsilon_{av}(L_{add})$ are given and analyzed. It is also significant that the average errors of solving self-connected problems of interpolation-extrapolation digital data for right-hand and left-hand asymmetric ravine functions aresimilar.

Obtained simulation results can be interesting for experts in the physics of electron beams, in the elaboration of HVGD electron guns, and in applying advanced electron-beam technologies in different branches of modern industry.

REFERENCES

1. J.D. Lawson, *The Physics of Charged-Particle Beams*. Oxford: Clarendon Press, 1977, 446 p. Available: https://www.semanticscholar.org/paper/The-Physics-of-Charged-Particle-Beams-Stringer/80b5ee5289d5efd8f480b516ec4bade0aa529ea6
2. M. Reiser, *Theory and Design of Charged Particle Beams*. John Wiley & Sons, 2008, 634 p. Available: https://www.wiley.com/en-us/Theory+and+Design+of+Charged+Particle+Beams-p-9783527617630
3. M. Szilagyi, *Electron and Ion Optics*. Springer Science & Business Media, 2012, 539 p. Available: https://www.amazon.com/Electron-Optics-Microdevices-Miklos-Szilagyi/dp/1461282470
4. S.J.R. Humphries, *Charged Particle Beams*. Courier Corporation, 2013, 834 p. Available: https://library.uoh.edu.iq/admin/ebooks/76728-charged-particle-beams---s.-humphries.pdf
5. S. Schiller, U. Heisig, and S. Panzer, *Electron Beam Technology*. John Wiley & Sons Inc, 1995, 508 p. Available: https://books.google.com.ua/books/about/Electron_Beam_Technology.html?id=QRJTAAAAMAAJ&redir_esc=y
6. R.A. Bakish, *Introduction to Electron Beam Technology*. Wiley, 1962, 452 p. Available: https://books.google.com.ua/books?id=GghTAAAAMAAJ&hl=uk&source=gbs_similarbooks
7. R.C., Davidson, H. Qin, *Physics of Intense Charged Particle Beams in High Energy Accelerators*. World Scientific, Singapore, 2001, 604 p. Available: https://books.google.com.ua/books/about/Physics_Of_Intense_Charged_Particle_Beam.html?id=5M02DwAAQBAJ&redir_esc=y
8. H. Schultz, *Electron Beam Welding*. Woodhead Publishing, 1993, 240 p. Available: https://books.google.com.ua/books?id=I0xMo28DwcIC&hl=uk&source=gbs_book_similarbooks
9. G. Brewer, *Electron-Beam Technology in Microelectronic Fabrication*. Elsevier, 2012, 376 p. Available: https://books.google.com.ua/books?idsnU5sOQD6noC&hl=uk&source=gbs_similarbooks
10. I. Brodie, J.J. Muray, *The Physics of Microfabrication*. Springer Science & Business Media, 2013, 504 p. Available: https://books.google.com.ua/books?id=GQYHCAAAQBAJ&hl=uk&source=gbs_similarbooks
11. A.A. Druzhinin, I.P. Ostrovskii, Y.N. Khoverko, N.S.Liakh-Kaguy, and A.M. Vuytsyk, "Low temperature characteristics of germanium whiskers," *Functional materials 21*, no. 2, pp. 130–136, 2014. Available: http://dspace.nbuv.gov.ua/bitstream/handle/123456789/120404/02-Druzhinin.pdf?sequence=1

12. A.A. Druzhinin, I.A. Bolshakova, I.P. Ostrovskii, Y.N. Khoverko, and N.S. Liakh-Kaguy, "Low temperature magnetoresistance of InSb whiskers," *Materials Science in Semiconductor Processing*, vol. 40, pp. 550–555, 2015. Available: https://academic-accelerator.com/search?Journal=Druzhinin
13. A. Zakharov, S. Rozenko, S. Litvintsev, and M. Ilchenko, "Trisection Bandpass Filter with Mixed Cross-Coupling and Different Paths for Signal Propagation," *IEEE Microwave Wireless Component Letters*, vol. 30, no. 1, pp. 12–15, Jan. 2020.
14. A. Zakharov, S. Litvintsev, and M. Ilchenko, "Trisection Bandpass Filters with All Mixed Couplings," *IEEE Microwave Wireless Components Letter*, vol. 29, no. 9, pp. 592–594, 2019. Available: https://ieeexplore.ieee.org/abstract/document/8782802
15. A. Zakharov, S. Rozenko, and M. Ilchenko, "Varactor-tuned microstrip bandpass filter with loop hairpin and combline resonators," *IEEE Transactions on Circuits Systems. II. Experimental Briefs*, vol. 66, no. 6, pp. 953–957, 2019. Available: https://ieeexplore.ieee.org/document/8477112
16. T. Kemmotsu, T. Nagai, and M. Maeda, "Removal Rate of Phosphorous form Melting Silicon," *High Temperature Materials and Processes*, vol. 30, issue 1-2, pp. 17–22, 2011. Available: https://www.degruyter.com/journal/key/htmp/30/1-2/html
17. J.C.S. Pires, A.F.B. Barga, and P.R. May, "The purification of metallurgically grade silicon by electron beam melting," *Journal of Materials Processing Technology*, vol. 169, no. 1, pp. 347–355, 2005. Available: https://www.academia.edu/9442020/The_purification_of_metallurgical_grade_silicon_by_electron_beam_melting
18. D. Luo, N. Liu, Y. Lu, G.Zhang, and T. Li, "Removal of impurities from metallurgically grade silicon by electron beam melting," *Journal of Semiconductors*, vol. 32, issue 3, article ID 033003, 2011. Available: http://www.jos.ac.cn/en/ article/doi/10.1088/1674-4926/32/3/033003
19. D. Jiang, Y. Tan, S. Shi, W. Dong, Z. Gu, and R. Zou, "Removal of phosphorous in molten silicon by electron beam candle melting," *Materials Letters*, vol. 78, pp. 4–7, 2012.
20. A.F. Tseluyko, V.T. Lazurik, D.L. Ryabchikov, V.I. Maslov, and I.N. Sereda, "Experimental study of radiation in the wavelength range 12.2-15.8 nm from a pulsed high-current plasma diode," *Plasma Physics Reports*, 34(11), pp. 963–968, 2008. Available: https://link.springer.com/article/10.1134/S1063780X0811010X
21. V.G. Rudychev, V.T. Lazurik, and Y.V. Rudychev, "Influence of the electron beams incidence angles on the depth-dose distribution of the irradiated object," *Radiation Physics and Chemistry*, 186, 109527, 2021. Available: https://www.sciencedirect.com/science/article/abs/pii/S0969806X21001778
22. V.M. Lazurik, V.T. Lazurik, G. Popov, and Z. Zimek, "Two-parametric model of electron beam in computational dosimetry for radiation processing, *Radiation Physics and Chemistry*, 124, pp. 230–234, 2016. Available: https://www.sciencedirect.com/science/article/abs/pii/S0969806X1530133X
23. I. Melnyk, S. Tuhai, and A. Pochynok, "Universal Complex Model for Estimation the Beam Current Density of High Voltage Glow Discharge Electron Guns," *Lecture Notes in Networks and Systems*; Eds: M. Ilchenko, L. Uryvsky, L. Globa, vol. 152, pp. 319–341, 2021. Available: https://www.springer.com/gp/book/9783030583583
24. S.V. Denbnovetsky, V.G. Melnyk, and I.V. Melnyk, "High voltage glow discharge electron sources and possibilities of its application in industry for realizing different technological operations," *IEEE Transactions on Plasma Science*, vol. 31, issue 5, pp. 987–993, October, 2003. doi: 10.1109/TPS.2003.818444
25. S. Denbnovetskiy et al., "Principles of operation of high voltage glow discharge electron guns and particularities of its technological application," *Proceedings of SPIE, The International Society of Optical Engineering*, pp. 10445–10455, 2017. Available: https://spie.org/Publications/Proceedings/Paper/10.1117/12.2280736
26. I.V. Melnyk, "Numerical simulation of distribution of electric field and particle trajectories in electron sources based on high-voltage glow discharge," *Radioelectronic and Communication Systems*, vol. 48, no. 6, pp. 61–71, 2005. doi: https://doi.org/10.3103/S0735272705060087

27. S.V. Denbnovetsky, J. Felba, V.I. Melnik, and I.V. Melnik, "Model of Beam Formation in a Glow Discharge Electron Gun with a Cold Cathode," *Applied Surface Science*, 111, pp. 288–294, 1997. Available: https://www.sciencedirect.com/science/ article/pii/S0169433296007611?via%3Dihub
28. J.I. Etcheverry, N. Mingolo, J.J. Rocca, and O.E. Martınez, "A Simple Model of a Glow Discharge Electron Beam for Materials Processing," *IEEE Transactions on Plasma Science*, vol. 25, no. 3, pp. 427–432, June, 1997.
29. S.V. Denbnovetsky, V.I. Melnyk, I.V. Melnyk, and B.A. Tugay, "Model of control of glow discharge electron gun current for microelectronics production applications," *Proceedings of SPIE. Sixth International Conference on "Material Science and Material Properties for Infrared Optoelectronics"*, vol. 5065, pp. 64–76, 2003. doi: https://doi.org/10.1117/12.502174
30. I.V. Melnyk, "Estimating of current rise time of glow discharge in triode electrode system in case of control pulsing," *Radioelectronic and Communication Systems*, vol. 56, no. 12, pp. 51–61, 2017.
31. A. Mitchell, T. Wang, "Electron beam melting technology review," *Proceedings of the Conference "Electron Beam Melting and Refining State of the Art 2000, Reno, NV, USA, 2000*, ed. R. Bakish, pp. 2–13.
32. D.V. Kovalchuk, N.P. Kondraty, "Electron-beam remelting of titanium – problems and development prospects," *Titan 2009*, no. 1(23), pp. 29–38.
33. V.A. Savenko, N.I. Grechanyuk, and O.V. Churakov, "Electron beam refining in production of platinum and platinum-base alloys. Information 1. Electron beam refining of platinum," *Advances in Electrometallurgy*, no. 1, pp. 14–16, 2008.
34. T.O. Prikhna et al., "Electron-Beam and Plasma Oxidation-Resistant and Thermal-Barrier Coatings Deposited on Turbine Blades Using Cast and Powder Ni(Co)CrALY(Si) Alloys I. Fundamentals of the Production Technology, Structure, and Phase Composition of Cast NiCrAlY Alloys," *Powder Metallurgy and Metal Ceramics*, vol. 61, issue 1-2, pp. 70–76, 2022. Available: https://link.springer.com/article/10.1007/s11106-022-00296-8
35. T.O. Prikhna et al., "Electron-Beam and Plasma Oxidation-Resistant and Thermal-Barrier Coatings Deposited on Turbine Blades Using Cast and Powder Ni(Co)CrAlY(Si) Alloys Produced by Electron-Beam Melting II. Structure and Chemical and Phase Composition of Cast CoCrAlY Alloys," *Powder Metallurgy and Metal Ceramicsthis*, vol. 61, issue 3-4, pp. 230–237, 2022.
36. I.M. Grechanyuk et al., "Electron-Beam and Plasma Oxidation-Resistant and Thermal-Barrier Coatings Deposited on Turbine Blades Using Cast and Powder Ni(Co)CrAlY(Si) Alloys Produced by Electron Beam Melting IV. Chemical and Phase Composition and Structure of Cocralysi Powder Alloys and Their Use," *Powder Metallurgy and Metal Ceramics*, vol. 61, issue 7-8, pp. 459–464, 2022.
37. M.I. Grechanyuk et al., "Electron-Beam and Plasma Oxidation-Resistant and Thermal-Barrier Coatings Deposited on Turbine Blades Using Cast and Powder Ni (Co)CrAlY (Si) Alloys Produced by Electron Beam Melting III. Formation, Structure, and Chemical and Phase Composition of Thermal-Barrier Ni(Co)CrAlY/ZrO_2–Y_2O_3 Coatings Produced by Physical Vapor Deposition in One Process Cycle," *Powder Metallurgy and Metal Ceramics*, vol. 61, issue 5-6, pp. 328–336, 2022.
38. J. Zhang et al., "Fine equiaxed β grains and superior tensile property in Ti–6Al–4V alloy deposited by coaxial electron beam wire feeding additive manufacturing," *Acta Metallurgica Sinica (English Letters)*, 33(10), pp. 1311–1320, 2020.
39. D. Kovalchuk, O. Ivasishin, "Profile electron beam 3D metal printing," in *Additive Manufacturing for the Aerospace Industry*. Elsevier Inc., 2019, pp. 213–233.
40. M. Wang et al., "Microstructure and mechanical properties of Ti-6Al-4V cruciform structure fabricated by coaxial electron beam wire-feed additive manufacturing," *Journal of Alloys and Compounds*, vol. 960. article 170943. doi: https://doi.org/10.1016/j.jallcom.2023.170943
41. I. Melnyk, S. Tuhai, M. Surzhykov, I. Shved, V. Melnyk, and D. Kovalchuk, "Analytical Estimation of the Deep of Seam Penetration for the Electron-Beam Welding Technologies with Application of Glow Discharge Electron Guns," *2022 IEEE 41-st International Conference on Electronics and Nanotechnology (ELNANO), 2022*, pp. 1–5.

42. I. Melnyk, S. Tuhai, and A. Pochynok, "Calculation of Focal Paramters of Electron Beam Formed in Soft Vacuum at the Plane which Sloped to Beam Axis," *The Forth IEEE International Conference on Information-Communication Technologies and Radioelectronics UkrMiCo'2019. Collections of Proceedings of the Scientific and Technical Conference, Odesa, Ukraine, September 9-13, 2019*. doi: 10.1109/UkrMiCo47782.2019.9165328
43. I. Melnyk, S. Tuhai, and A. Pochynok, "Interpolation of the Boundary Trajectories of Electron Beams by the Roots from Polynomic Functions of Corresponded Order," *2020 IEEE 40th International Conference on Electronics and Nanotechnology (ELNANO)*, pp. 28–33. doi: 10.1109/ELNANO50318.2020.9088786
44. I. Melnik, S. Tugay, and A. Pochynok, "Interpolation Functions for Describing the Boundary Trajectories of Electron Beams Propagated in Ionised Gas," *15-th International Conference on Advanced Trends in Radioelectronics, Telecommunications and Computer Engineering (TCSET – 2020)*, pp. 79–83. doi: 10.1109/TCSET49122.2020.235395
45. I.V. Melnyk, A.V. Pochynok, "Study of a Class of Algebraic Functions for Interpolation of Boundary Trajectories of Short-Focus Electron Beams," *System Researches and Information Technologies*, no. 3, pp. 23–39, 2020. doi: https://doi.org/10.20535/SRIT.2308-8893.2020.3.02
46. I. Melnyk, S. Tuhai, M. Skrypka, A. Pochynok, and D. Kovalchuk, "Approximation of the Boundary Trajectory of a Short-Focus Electron Beam using Third-Order Root-Polynomial Functions and Recurrent Matrixes Approach," *2023 International Conference on Information and Digital Technologies (IDT)*, Zilina, Slovakia, 2023, pp. 133–138, doi: 10.1109/IDT59031.2023.10194399
47. I. Melnyk, A. Luntovskyy, "Estimation of Energy Efficiency and Quality of Service in Cloud Realizations of Parallel Computing Algorithms for IBN," in Klymash, M., Beshley, M., Luntovskyy, A. (eds) *Future Intent-Based Networking. Lecture Notes in Electrical Engineering*, vol. 831, Springer, Cham, pp. 339–379. doi: https://doi.org/10.1007/978-3-030-92435-5_20
48. G.M. Phillips, *Interpolation and Approximation by Polynomials*. Springer, 2023, 312 p. Available: http://bayanbox.ir/view/2518803974255898294/George-M.-Phillips-Interpolation-and-Approximation-by-Polynomials-Springer-2003.pdf
49. N. Draper, H. Smith, *Applied Regression Analysis*; 3 Edition. Wiley Series, 1998, 706 p. Available: https://www.wiley.com/en-us/Applied+Regression+ Analysis,+3rd+Edition-p-9780471170822
50. C. Mohan, K. Deep, *Optimization Techniques*. New Age Science, 2009, 628 p. Available: https://www.amazon.com/Optimization-Techniques-C-Mohan/dp/1906574219
51. M.K. Jain, S.R.K. Iengar, and R.K. Jain, *Numerical Methods for Scientific & Engineering Computation*. New Age International Pvt. Ltd., 2010, 733 p. Available: https://www.google.com.ua/url?sa=t&rct=j&q=&esrc=s&source=web&cd=&ved=2ahUKEwippcuT7rX8AhUhlYsKHRfBCG0QFnoECEsQAQ&url=https%3A%2F%2Fwww.researchgate.net%2Fprofile%2FAbiodun_Opanuga%2Fpost%2Fhow_can_solve_a_non_linear_PDE_using_numerical_method%2Fattachment%2F59d61f7279197b807797de30%2FAS%253A284742038638596%25401444899200343%2Fdownload%2FNumerical%2BMethods.pdf&usg=AOvVaw0MjNl3K877lVWUWw-FPwmV
52. S.C. Chapra, R.P. Canale, *Numerical Methods for Engineers*; 7th Edition. McGraw Hill, 2014, 992 p. Available: https://www.amazon.com/Numerical-Methods-Engineers-Steven-Chapra/dp/007339792X
53. E. Wentzel, L. Ovcharov, *Applied Problems of Probability Theory*. Mir, 1998, 432 p. Available: https://mirtitles.org/2022/06/03/applied-problems-in-probability-theory-wentzel-ovcharov/
54. J.A. Gubner, *Probability and Random Processes for Electrical and Computer Engineers*. UK, Cambridge: Cambridge University Press, 2006. Available: http://www.amazon.com/Probability-Processes-Electrical-Computer-Engineers/dp/0521864704
55. M. Lutz, *Learning Python*; 5th Edition. O'Reilly, 2013, 1643 p.
56. W. McKinney, *Python for Data Analysis: Data Wrangling with Pandas, NumPy, and Jupyter*; 3rd Edition. O'Reilly Media, 2023, 579 p.

Received 02.11.2023

INFORMATION ON THE ARTICLE

Igor V. Melnyk, ORCID: 0000-0003-0220-0615, National Technical University of Ukraine "Igor Sikorsky Kyiv Polytechnic Institute", Ukraine, e-mail: imelnik@phbme.kpi.ua

Alina V. Pochynok, ORCID: 0000-0001-9531-7593, Research Institute of Electronics and Microsystem Technology of the National Technical University of Ukraine "Igor Sikorsky Kyiv Polytechnic Institute", Ukraine, e-mail: alina_pochynok@yahoo.com

Mykhailo Yu. Skrypka, ORCID: 0009-0006-7142-5569, National Technical University of Ukraine "Igor Sikorsky Kyiv Polytechnic Institute", Ukraine, e-mail: scientetik@gmail.com

ПОРІВНЯННЯ ЗАСТОСУВАННЯ МЕТОДІВ ІНТЕРПОЛЯЦІЇ ТА ЕКСТРАПОЛЯЦІЇ ГРАНИЧНИХ ТРАЄКТОРІЙ КОРОТКОФОКУСНИХ ЕЛЕКТРОННИХ ПУЧКІВ ІЗ ВИКОРИСТАННЯМ КОРЕНЕВО-ПОЛІНОМІАЛЬНИХ ФУНКЦІЙ / І.В. Мельник, А.В. Починок, М.Ю. Скрипка

Анотація. Розглянуто й обговорено порівняння методів інтерполяційного та екстраполяційного оцінювання граничної траєкторії електронних пучків, які поширюються в іонізованому газі. Оцінювання виконано з використанням коренево-поліноміальних функцій для числового розв'язання системи алгебро-диференціальних рівнянь, що описують граничну траєкторію електронного пучка. Показано та доведено, що у разі розв'язання взаємозв'язаної задачі інтерполяції-екстраполяції середня похибка оцінювання радіуса променя, зазвичай, є меншою. Особливо ефективним виявилося використання цього підходу в оцінюванні фокального радіуса променя. Наведено алгоритм розв'язання інтерполяційно-екстраполяційної задачі та пояснено його ефективність. Наведено та проаналізовано відповідні графічні залежності.

Ключові слова: інтерполяція, екстраполяція, коренево-поліноміальна функція, яружна функція, електронний пучок, гранична траєкторія.